

Structural investigation of the adsorption of SnPc on Ag(111) using normal-incidence x-ray standing waves

C. Stadler,* S. Hansen, F. Pollinger, C. Kumpf, and E. Umbach
Experimentelle Physik II, Universität Würzburg, Am Hubland, D-97074 Würzburg, Germany

T.-L. Lee and J. Zegenhagen
European Synchrotron Radiation Facility, Boîte Postale 220, F-38043 Grenoble Cedex, France
 (Received 20 January 2006; revised manuscript received 24 April 2006; published 6 July 2006)

The bonding of tin(II)-phthalocyanine (SnPc) on Ag(111) was studied using the normal incidence x-ray standing wave technique. For an incommensurate monolayer structure at room temperature, it was found that the SnPc molecules adsorb in a “Sn-down” geometry, i.e., the Sn atoms lie below the molecular plane. A significant bending of the benzene rings toward the surface indicates that these rings contribute to a chemisorptive bonding of the molecule to the surface. This effect is found to be even enhanced for another phase, a commensurate submonolayer structure that is only stable at low temperature. In this phase, the molecules are located significantly closer to the surface in a mixed “Sn-up”-“Sn-down” configuration. Nondipolar contributions to the photoelectron yield were also investigated and taken into account.

DOI: [10.1103/PhysRevB.74.035404](https://doi.org/10.1103/PhysRevB.74.035404)

PACS number(s): 68.49.Uv

I. INTRODUCTION

During the last several years, the adsorption of large organic molecules on metal surfaces has attracted much interest of the surface science community. Many activities deal with the investigation of the interaction between the first layer adsorbate molecules and the substrates, since this interaction determines the structural ordering of the organic films and therefore also the optical, electronic, and magnetic properties of the system.¹⁻⁴ Usually, a long-range ordered overlayer can only be obtained in the case of physisorbed or weakly chemisorbed monolayers. Within these boundaries, however, a wide range of different adsorption behaviors can occur. In general, the bulk properties are the more important for the formation of an organic film the weaker the adsorbate-substrate interaction is, since the molecule-molecule interaction plays the dominant role in this case. For a long time, the adsorbate-substrate interaction had been considered to be generally weak (“physisorption”) for organic adsorbates on metallic substrates until recently several examples of much stronger interactions were reported (see Refs. 5-12, and references therein).

Meanwhile, there is also an increasing interest of theoretical groups in this field, who urgently need accurate structural information, such as atomic positions and bonding distances in order to develop and improve their quantum chemical model calculations. The most important parameter for the calculations is the precise height of the adsorbate molecule and its atoms above the substrate surface. As demonstrated by several recent publications, the normal incidence x-ray standing wave (NIXSW) technique is well suited for providing such information.¹³⁻¹⁹ In ideal cases even a full determination of the adsorbate site is possible by NIXSW via triangulation.¹⁶⁻¹⁹

The subject of this work is the adsorption of tin(II)-phthalocyanine (SnPc) on the Ag(111) surface. SnPc is a nonplanar representative of the metal-phthalocyanines that has not been very intensively investigated so far. A schematic

picture of the molecule is shown in Fig. 1. In contrast to planar molecules of this family, such as the most prominent CuPc, SnPc is significantly “bent” in the gas phase since the Sn atom does not lie in the molecular plane. Therefore, it can, in principle, adsorb in two different flat-lying geometries: with the Sn atom either below (Sn-down) or above the molecular plane (Sn-up). The phase diagram for the adsorption of this molecule on Ag(111) is still under investigation.²⁰⁻²³ In this paper, we present NIXSW results on two prominent phases: At first, an incommensurate monolayer with one molecule per unit cell was investigated at room temperature (RT). This phase can be prepared easily by annealing a multilayer film of SnPc at about 290 °C. The resulting monolayer is saturated, which is defined as coverage 1 (=100% = 1 ML). The second structure is a commensurate submonolayer structure with two molecules per unit cell.

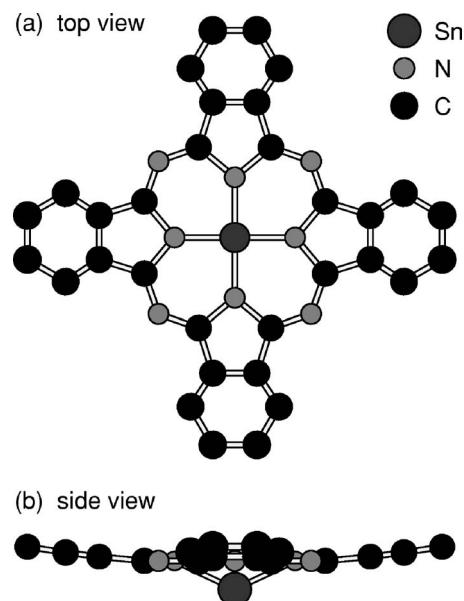


FIG. 1. Schematic picture of the free SnPc molecule.

This phase only exists at temperatures below 230 K, and the corresponding room-temperature phase is disordered. Note, that this low temperature (LT) phase is identical to the so-called dense packing of SnPc on Ag(111) in Refs. 22 and 23. Further details on these and other phases are given in Refs. 20–23. For both structures, we here determine the precise adsorption heights above the Ag surface of all atomic species in the molecule (Sn, C, and N) by NIXSW experiments. We show that for the incommensurate RT phase the molecules adsorb in Sn-down position, whereas the commensurate LT phase consists of a mixed Sn-up and Sn-down configuration. Additionally, a significant bending of the benzene rings toward the surface is found.

II. THE XSW TECHNIQUE

In an x-ray standing wave (XSW) experiment, very precise atomic positions of adatoms can be obtained by measuring the relative x-ray absorption of these atoms as a function of photon energy or angle. When the Bragg condition for a $\mathbf{H}=(hkl)$ reflection of the substrate crystal is fulfilled, the incident and the Bragg-reflected x-ray waves form a standing wave field perpendicular to the Bragg planes, which has the spatial modulation of the corresponding Bragg plane spacing $d_{\mathbf{H}}$. As one scans, e.g., the photon energy in a certain range close to the Bragg condition, the standing wave field moves by half of this distance $d_{\mathbf{H}}$ through the crystal due to its phase shift π . Therefore, the intensity of the electromagnetic field at a specific site, e.g., the adsorption site of an atom on the surface, varies in a characteristic way with the photon energy, depending on the distance of the atom to the Bragg planes. The atomic absorption $I(E)$ is proportional to this intensity profile of the x-rays and can be obtained experimentally by measuring either the photoelectron emission yield or the (subsequent) x-ray fluorescence or Auger electron emission yield. As a consequence, the measurement is sensitive to the considered atomic species. $I(E)$ can be calculated (and hence fitted to the experimental data) using dynamical diffraction theory.²⁴ For the intensity profile, one obtains^{18,25}

$$I(E) = 1 + R + 2\sqrt{R}F^{\mathbf{H}} \cos(\Phi + 2\pi P^{\mathbf{H}}), \quad (1)$$

where $R=R(E)$ is the reflectivity and $\Phi=\Phi(E)$ the phase of the standing wave field. The first two terms represent the incoherent sum of the incident and scattered waves, and the third term corresponds to the interference between the two waves. The so-called coherent position $P^{\mathbf{H}}=\frac{D^{\mathbf{H}}}{d_{\mathbf{H}}}$ and coherent fraction $F^{\mathbf{H}}$ are the structural parameters, which can be obtained from a fit to the measured absorption profile.

In the case of single site adsorption, $D^{\mathbf{H}}$ is the distance (modulo $d_{\mathbf{H}}$) between the atoms on this site and the Bragg planes for the reflection \mathbf{H} , and $F^{\mathbf{H}}$ is just equal 1. In the more general case of different inequivalent adsorption sites for the same element, $D^{\mathbf{H}}$ is the average of the distances between the atoms on these sites and the Bragg planes. $F^{\mathbf{H}}$ then is the contrast of the interference term that corresponds to the incoherent average of the contributions of all atoms to the absorption yield.

These two parameters $F^{\mathbf{H}}$ and $P^{\mathbf{H}}$ can also be understood as the amplitude and phase of the \mathbf{H} -Fourier component of the spatial distribution of an adsorbate. This interpretation allows a simple possibility to calculate the coherent position and fraction from an atomic model with several inequivalent adsorption sites for the same type of atoms. Every atom k that contributes to the absorption profile has a coherent fraction of $F_k^{\mathbf{H}}=1$ and an individual position $P_k^{\mathbf{H}}$. The signal measured for such a multisite adsorption system can then be described by the structural parameters $P^{\mathbf{H}}$ and $F^{\mathbf{H}}$, which are calculated by averaging all these complex numbers,

$$F^{\mathbf{H}} \exp(i2\pi P^{\mathbf{H}}) = \sum_{k=1}^N \frac{F_k^{\mathbf{H}}}{N} \exp(i2\pi P_k^{\mathbf{H}}). \quad (2)$$

It is often convenient to present this complex quantity in polar coordinates (Argand diagram), where the absolute value (length of the vector) is the coherent fraction and the phase (angle of the vector with respect to the real axis) corresponds to the coherent position, i.e., a phase of 2π corresponds to the distance $d_{\mathbf{H}}$.

In this paper, the photoelectron (PE) yield is used to measure the XSW absorption profiles. Usually, the dipole approximation is used to describe the photoemission process, an approximation that is valid if the wavelength of the incident beam is large compared to the spatial dimensions of the involved orbitals as in the case of UV radiation. In the present case, however, higher multipole contributions to the PE yield are no longer negligible due to the much shorter wavelength.^{26–28} Thus, PE multipole contributions have to be considered, in the case of the XSW technique for both the incoming and Bragg-reflected wave, which are coherent. Their effect can be considered by introducing correction parameters in Eq. (1). Usually, magnetic dipole and the electronic quadrupole contributions to the photoelectron yield are taken into account, which changes Eq. (1) to^{26–28}

$$I(E) = 1 + \frac{1+Q}{1-Q}R + 2\sqrt{R}F^{\mathbf{H}} \frac{(1+Q^2 \tan^2 \Delta)^{1/2}}{1-Q} \times \cos(\Phi - \Psi + 2\pi P^{\mathbf{H}}). \quad (3)$$

Equation (3) contains the nondipolar parameters Q , Δ , and $\Psi=\tan^{-1}(Q \tan \Delta)$. In the present study, the asymmetry parameter Q is determined from a multilayer of SnPc molecules, for which the coherent fraction vanishes due to the many atomic positions averaging incoherently. In this case the absorption profile reduces to

$$I(E) = 1 + \frac{1+Q}{1-Q}R, \quad (4)$$

and Q can easily be obtained from comparing the measured absorption yield and the reflectivity. Note that Q can also be calculated from the angular distribution of the PE process considering the specific orbital involved.^{29,30} The parameter Δ represents a relatively small correction. In the case of emission from an s -orbital Δ is the difference of the phases of the (dipole-excited) p - and (quadrupole-excited) d -electron waves. Theoretical values are available in this case,³¹ however, for emission from p - or d -states, no theory is es-

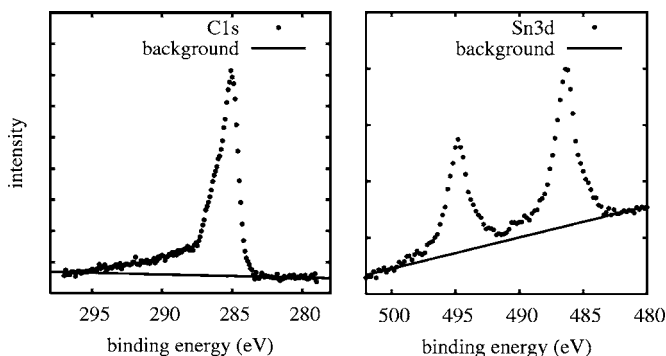


FIG. 2. Typical photoelectron spectra of the C1s (left) and Sn3d (right) of crystal A with a monolayer SnPc at room temperature.

tablished so far.²⁸ More details about the (NI)XSW technique and nondipolar contributions can be found in Refs. 13, 18, and 24–28.

III. EXPERIMENTAL

The experiments were carried out at beamline ID32 of the European Synchrotron Radiation Facility (ESRF) in Grenoble, France. The UHV surface science end-station of this beamline is equipped with a hemispherical electron analyzer ($r=150$ mm), a low-energy electron diffraction (LEED) optics, and facilities for sample preparation. The angle between the synchrotron beam and the analyzer axis was 45° . The base pressure of the chamber was below 5×10^{-10} mbar.

A. Sample preparation

In order to verify our results, we performed all experiments with two different Ag(111) crystals (A and B), which were mounted next to each other on the manipulator and prepared simultaneously. The experimental full widths at half maximum (FWHM) of the Ag(111) reflectivity curves are 1.06 and 1.15 eV for crystals A and B, respectively. If not mentioned explicitly, all results refer to both crystals.

The crystals were cleaned and annealed following a standard procedure. Afterward the surface cleanliness was checked with XPS, and the cleaning procedure repeated until no C1s photoelectron peak could be detected any more. Subsequently, the SnPc layers were prepared by evaporating SnPc while the Ag crystal was kept at RT.

Three different structures were prepared: a relatively thick multilayer, an incommensurate room-temperature monolayer structure with one molecule per unit cell, and a low-temperature commensurate submonolayer phase with two molecules per unit cell. The last structure is disordered at room temperature, but orders upon cooling below 230 K and shows sharp LEED spots.

The multilayer structure was prepared by evaporation of SnPc for 10 min. No Ag3d XPS could be detected through the multilayer at a photon energy of 2.63 keV. Using this preparation, the asymmetry parameters Q for all different atomic species (C1s, N1s, Sn3d) were measured on three different spots on crystal A with an acquisition time of ~ 45 min per spot.

Afterward, the samples were annealed at 290°C to desorb the multilayers. This procedure is known to result in a compressed monolayer structure, which was already investigated by scanning tunneling microscopy (STM)^{22,23} and high-resolution (spot profile analysis) low energy electron diffraction (SPA)LEED.^{20,21} This structure is stable at room temperature and shows very bright and sharp LEED spots, which were used to check the preparation.

After taking data on both crystals, the samples were cleaned and the submonolayer structure was prepared. Since this structure is only stable below 230 K for coverages between 0.68 and 0.88 ML,²¹ approximately 0.1 ML of SnPc was deposited on the silver crystal several times with an adsorption rate of <0.03 ML/min. After each evaporation step, the structure was checked at low temperature (below 230 K). This was repeated until the pure commensurate phase formed on crystal B. In another attempt, an even better preparation could be obtained on crystal A. The XSW results obtained at 150 K from these two preparations will be presented below. By comparing the C1s intensities with those measured from the saturated RT phase, we determined the coverage for the LT phase to be 0.87 ML for crystal A and 0.78 ML for crystal B.

B. Data acquisition and raw data treatment

In this work, the NIXSW absorption profiles of three different regions of interest, C1s, N1s, and Sn3d, were measured as a function of the photon energy near the Ag(111) Bragg energy (2627 eV). Absorption profiles of the bulk Ag were also measured for the clean crystal as well as for all adsorbate-induced superstructures. As expected from earlier experiments,^{13,16} very high coherent fractions (>0.9) were obtained from the Ag signals (not shown). This indicates that no distortions of the uppermost Ag layers are present. The photon energy scan range was 8–10 eV with 50–60 points per XSW scan. The typical scan time for one scan was 10–30 min, and the time on each spot of the sample 45–120 min. Simultaneously to the measurements of the absorption profiles, the intensity of the incoming and the Bragg-reflected beam as well as the total electron yield (sample current) were recorded.

Possible beam damage was monitored by comparing the XPS spectra before and after each NIXSW run, and no

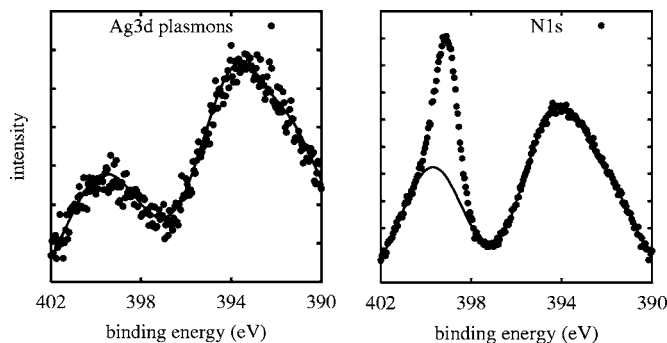


FIG. 3. Typical photoelectron spectra of the N1s region: the clean silver crystal with the Ag3d plasmons (left) and with a monolayer SnPc at room temperature (right).

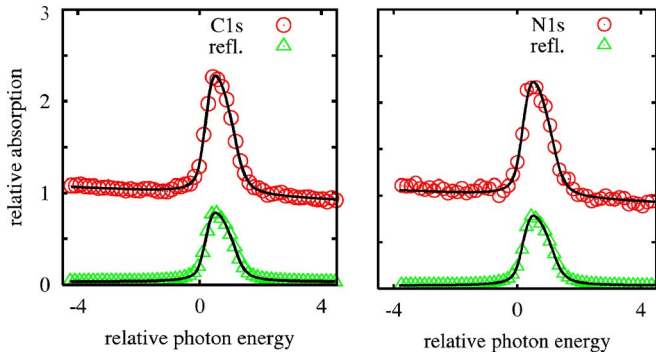


FIG. 4. (Color online) XSW scans of the incoherent multilayer. The C1s and N1s PES yields and the reflectivity curves are shown.

changes could be detected. Additional checks using LEED after each NIXSW measurement also confirmed the stability of the superstructures.

One important step in the raw data treatment is the proper handling of the background of the photoelectron spectra. In the case of C1s and Sn3d (Fig. 2) a linear background was sufficient. For the N1s yield, a polynomial fit for the background was needed, since some Ag3d plasmons occur in this region (continuous lines in Fig. 3). In all cases, we integrated the peak intensities and normalized them to the intensity of the incoming photon beam in order to compute the absorption profiles. Subsequently, the absorption profile of each scan was fitted, and thus several (up to 17) values for the coherent fraction and coherent position were obtained. For comparison, we also analyzed the properly averaged raw data. The fit parameters obtained from this analysis match within the error bars the mean values found in the analysis of individual curves. This does not hold for N1s, where the statistics of a single run is too poor to subtract correctly the relatively complicated background of the Ag3d plasmons, in particular, for those energies where the N1s signal is low. Therefore, for N1s only the results of the averaged signals are discussed in the following.

IV. RESULTS AND DISCUSSION

A. Multilayer structure

The goal of measuring XSW of the SnPc multilayer was to determine the nondipolar parameters Q for all atomic species. As described above [see Eq. (4)], Q can be determined by comparing the absorption profile and the reflectivity if the

TABLE I. Nondipolar parameters: Q values are derived from the linearly corrected fits of the multilayer data for the (111) Bragg reflection on crystal A using Eq. (4). The values for Δ are taken from Ref. 31. Note that values for Δ are only available for emission from s -orbitals at present.²⁸

	C1s	N1s	Sn3d
Q	0.24(2)	0.22(2)	0.17(2)
Δ	-0.21	-0.26	

coherent fraction is known to vanish as is the case for sufficiently thick multilayers. The best fits to the N1s and C1s XSW curves are shown in Fig. 4, the results of all fits are listed in Table I. We mention that the overall intensity showed a small linear decrease with increasing energy, indicated by a slightly changing background (see Fig. 4). This effect can be corrected with a linear scaling factor for the intensity which changes the fit result of the Q value by less than 0.02. This value can hence be considered as an error bar for Q . The results obtained for Q are in quite good agreement with previous experiments^{13,14} and theoretical calculations.^{29,32} It should be mentioned that for all atomic species, even for Sn, a rather big value for Q is obtained, which indicates that multipole corrections have to be considered even for relatively heavy atoms, for which they are often neglected so far. Therefore also for the Ag3d-based XSW-measurement nondipolar parameters should be considered. A Q parameter close to the value for Sn3d could be used since the angular distribution of the PE process is similar for Ag3d and Sn3d.²⁹ However, when the coherent position is close to 0 (which is the case for our Ag bulk crystal) the XSW curve is hardly affected by the Q parameter. Varying Q in the range of 0–0.3 changes the coherent fraction only by a few percent.

B. Incommensurate monolayer structure at RT

The incommensurate monolayer structure at room temperature was measured on both crystals, which yielded very similar results. The absorption profiles were fitted using Eq. (3) with the Q and Δ values from Table I. Typical XSW scans and fits to the XSW profiles are shown in Fig. 5. The results of the fits of all individual scans are presented in an Argand diagram in Fig. 6. The D^H and F^H values obtained from the averaged signals are listed in Table II. In Fig. 7(a), we present a schematic model showing the average distances of all atomic species, assuming that the molecules adsorb in

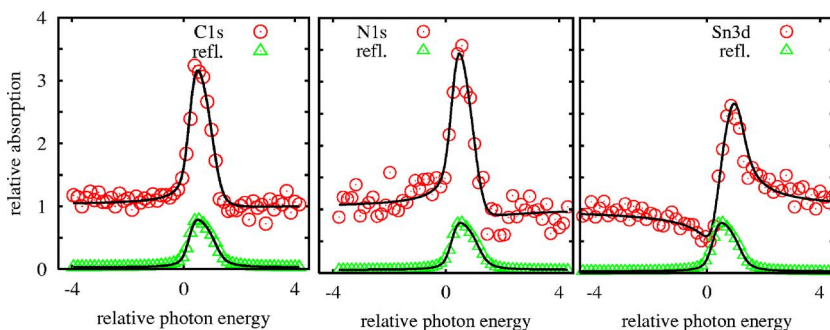


FIG. 5. (Color online) XSW scans of the incommensurate monolayer structure on crystal A. C1s, N1s, and Sn3d PES yields and reflectivity curves are shown.

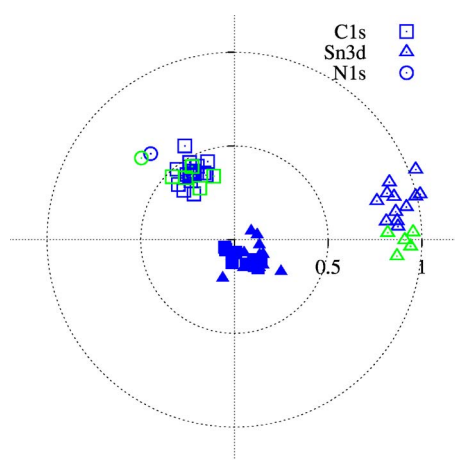


FIG. 6. (Color online) Argand diagram of the XSW results obtained from the monolayer structure at room temperature. Blue (dark) symbols represent the measurements on crystal A, green (light) symbols correspond to crystal B. Open symbols are results from the (111) Bragg reflection, full symbols from the $(\bar{1}\bar{1}\bar{1})$ Bragg reflection.

a planar geometry. The most prominent result is that the Sn atoms are located about 0.8 \AA below the carbon and nitrogen atoms, i.e., all molecules adsorb in a Sn-down configuration on the surface. Since very high coherent fractions are found for Sn3d all tin atoms adsorb at the same height above the Ag substrate surface. The fact that this height is very close to the Ag(111) Bragg plane spacing (2.36 \AA) raises the question whether the Sn atoms occupy bulklike positions in or above the uppermost silver layer. It might even be possible, that the Sn atoms dissociate from the Pc molecules and diffuse deeply into the Ag bulk crystal or adsorb independently on the Ag surface. This can be checked by performing XSW scans along the $(\bar{1}\bar{1}\bar{1})$ reflection, the Bragg planes of which are not parallel to the surface. If Sn occupies only bulk Ag sites, $F^{\bar{1}\bar{1}\bar{1}}$ should be as high as F^{111} , if Sn remains attached to the organic molecule $F^{\bar{1}\bar{1}\bar{1}}$ should drop drastically since the superstructure is incommensurate. The fit results of the $(\bar{1}\bar{1}\bar{1})$ measurements are shown in Table III and Fig. 6 (as full symbols). Almost all values obtained for the coherent fraction are below 0.2, whereas the coherent positions have values between 1.65 and 2.60 \AA . It is even possible to obtain a reasonable fit to the XSW data by using Eq. (4), which implies a coherent fraction of 0. This indicates that the Sn atoms do not occupy bulk Ag positions and particularly do not diffuse

TABLE II. Values for the coherent position and coherent fraction of the incommensurate monolayer phase at room temperature for the (111) Bragg reflection fitted using Eq. (3).

	Crystal	C1s	N1s	Sn3d
D^H [\AA]	A	3.16(3)	3.24(6)	2.46(3)
D^H [\AA]	B	3.17(3)	3.27(7)	2.36(3)
F^H	A	0.46(3)	0.64(12)	0.85(5)
F^H	B	0.42(4)	0.66(15)	0.90(5)

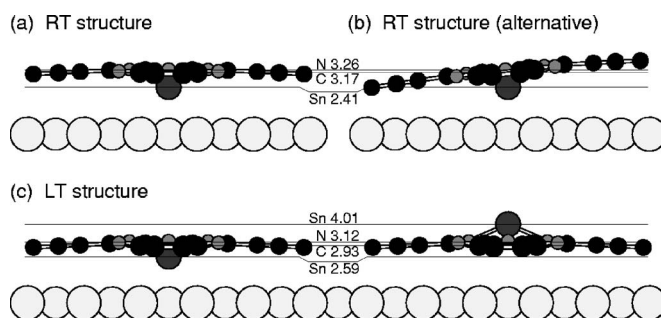


FIG. 7. Schematic models of the adsorption geometries for (a, b) the incommensurate RT structure and (c) the commensurate LT structure. Note that (a, b) shows two possible, alternative scenarios, while (c) shows two different geometries which occur in the same structure. Numbers represent the height of the corresponding atomic species above the uppermost bulk atomic plane in angstroms. For the RT structure, the values correspond to the average of the obtained values for the crystals A and B, for the LT structure the results for crystal A are shown.

into the bulk. The small Sn-Ag distance rather indicates a relatively strong interaction of the SnPc molecule with the Ag surface.

Another interesting aspect has to be mentioned: The height difference between the carbon atoms and the Sn atoms is rather small ($\approx 0.75 \text{ \AA}$), smaller than for a free molecule in the gas phase, which has no interaction to a surface. We also found a slightly larger distance from the surface for the nitrogen atoms than for the carbon atoms (see Table II). This indicates a significant “back bending” of the molecule, i.e., the outer benzene rings are bent toward the silver surface forming an “umbrella.” This bending of the molecule is a clear indication for a relatively strong bonding, i.e., chemisorption, between the molecule, especially the benzene rings, and the Ag surface, a result that is also confirmed by high resolution PES measurements.³³

A comparison of the coherent fractions for the atomic species also supports chemisorptive bonding: The tin atoms (only one adsorption site) show the highest coherent fraction (≈ 0.88). F^{111} for N1s is smaller (≈ 0.65), but still significantly higher than for C1s (≈ 0.44). Therefore, one can conclude that the positions of the carbon atoms are spread over a larger range of heights than for the nitrogen atoms. This finding is in agreement with the significant bending of the wings of the molecule, which was found from the comparison of the coherent positions for C and N (see above).

In order to check this aspect more quantitatively, one can assume a Gaussian distribution for the heights of carbon and nitrogen atoms. Then, the reduction of F^{111} from Sn3d to

TABLE III. Values for the coherent position and fraction of the incommensurate monolayer phase at room temperature. The values were obtained from crystal A using the $(\bar{1}\bar{1}\bar{1})$ Bragg reflection.

	Crystal	C1s	Sn3d
D^H [\AA]	A	1.9	2.07
F^H	A	0.12	0.14

TABLE IV. Values of the coherent position and fraction obtained for the commensurate submonolayer phase at 150 K on the (111) Bragg reflection fitted using Eq. (3).

	Crystal	C1s	N1s	Sn3d
D^H [Å]	A	2.93(6)	3.12(7)	4.48(5)
D^H [Å]	B	2.99(4)	3.02(4)	4.32(3)
F^H	A	0.57(8)	0.76(19)	0.29(4)
F^H	B	0.57(5)	0.69(11)	0.41(3)

C1s (N1s) would correspond to a distribution of the C (N) atoms with a FWHM of 1.2 Å (0.8 Å). These values, which appear to be quite high at first glance, can be explained by different scenarios. One possibility is, that the SnPc molecules lie not perfectly flat on the surface. In order to explain the difference in the coherent fractions of C, N, and Sn *only* with such a tilted adsorption position (i.e., ignore other reasons for a vertical disorder), a maximum tilt angle of 7° had to be considered for the molecule. This scenario is illustrated in Fig. 7(b). Note that the numbers given in these schematics are the *average* distances between the atomic species and the surface. Therefore, they are identical for the planar model shown in Fig. 7(a) and the tilted model in Fig. 7(b).

Another reason for the relatively small coherent fractions could be a stronger bending of the benzene “wings” [stronger than it is illustrated in Fig. 7(a)], maybe even a different bending of the four wings within one molecule. This bending could also be dynamic, thermally induced, a possibility that is compatible with higher coherent fractions found for the LT phase, which is discussed in Sec. IV C. A further alternative is a thermally activated frustrated rotation of the whole molecule leading to an average tilt angle as sketched by Fig. 7(b). Furthermore, an additional (probably smaller) contribution could stem from the fact that the superstructure is incommensurate and therefore has many different adsorption sites for the molecules. From the present data, we cannot unambiguously decide for a specific scenario, but we can argue that in all other experimental investigations available so far [STM,^{22,23} SPA-LEED,^{20,21} and high-resolution PES and NEXAFS (Ref. 33)] there are no indications for a static tilt of the molecules. Therefore, considering the resolution of these methods, one can conclude that the tilt of the molecules is (probably far) below 5°.

In conclusion, in the incommensurate monolayer structure we find that the SnPc molecules are adsorbed in Sn-down position on the Ag(111) surface with the outer benzene rings significantly bent back to the surface due to a chemisorptive bonding to the Ag surface. The data allow one to exclude a tilt of the molecules of more than 5°.

C. Commensurate submonolayer structure at LT

The most prominent difference between the results from the LT submonolayer structure and those from the saturated RT monolayer structure concerns the Sn absorption profiles (see Table IV and Fig. 8). Besides a change in the position, there is also a significant drop of the coherent fraction, even

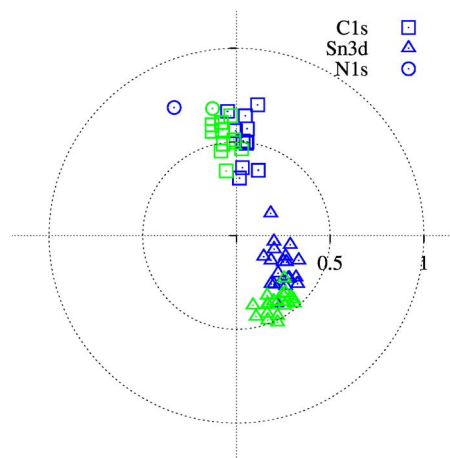


FIG. 8. (Color online) Argand diagram of the XSW results obtained from the commensurate submonolayer at 150 K. Blue (dark) symbols represent measurements on crystal A, green (light) symbols correspond to crystal B.

below the coherent fractions of the other atoms. This can only be explained by a model with (at least) two different adsorption geometries, a possibility that has already been discussed by Lackinger *et al.*^{22,23} The most obvious geometry is that one molecule of the unit cell is adsorbed in a Sn-up, the other one in a Sn-down configuration. If other possible reasons for disorder are ignored, the Sn-Ag distances can be calculated by averaging over both positions in the Argand diagram (see Fig. 9). Assuming further that both Sn adsorption geometries are equally occupied (two molecules per unit cell) and have a coherent fraction of 0.9 (only slightly smaller than the value obtained for Ag), positions of 2.59 Å (2.37 Å) for Sn-down and 4.01 Å (3.91 Å) for Sn-up are obtained from the measurements on crystal A (B) (see also Table V). A schematic model for the resulting adsorption geometry is shown in Fig. 7(c). Note that the distance between the Sn atoms and the rest of the molecule is smaller

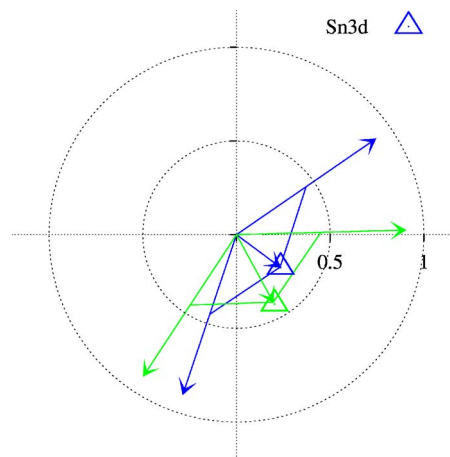


FIG. 9. (Color online) Argand diagram of the XSW results of the Sn atoms obtained from the commensurate submonolayer structure at 150 K. Blue (dark) symbols represent measurements on crystal A, green (light) symbols correspond to crystal B. The arrows indicate the positions of the Sn-up and Sn-down atoms.

TABLE V. Calculated values of the Sn-up and Sn-down positions for the commensurate submonolayer phase at 150 K. An occupation of 50% for both geometries and a coherent fraction of 0.9 is assumed (see also Fig. 9).

	Crystal	Sn-down	Sn-up
D^H [Å]	A	2.59	4.01
D^H [Å]	B	2.37	3.91

for the molecule in Sn-down-position (left) compared to the Sn-up position (right). The reason is a stronger interaction of the molecules with the substrate in this LT phase, which pulls the molecule closer to the surface and hence pushes the Sn atom towards the molecular plane, see the discussion below.

Even though the precise heights for the Sn atoms cannot unambiguously be derived from our data, the low coherent fractions found for the Sn3d PES signals clearly indicate that (at least) two adsorption heights are present for this superstructure, since a simple distortion of the molecules or additional molecular disorder would also reduce the coherent fractions of the other atoms. Their coherent fractions, however, are found to increase compared to those of the saturated RT monolayer structure, which indicates that the positions of these atoms are less different (see Table IV). Assuming again a Gaussian distribution for C and N atoms, the higher F^{111} values lead to a narrower distribution with a FWHM of 1.0 Å (0.6 Å) for the C (N) atoms, suggesting a smaller bending and/or a higher lateral order of the molecules compared to the saturated RT monolayer structure. Moreover, significantly reduced coherent positions (up to 0.2 Å) of the C and N atoms indicate a stronger bonding of the molecules to the Ag surface in the commensurate LT submonolayer structure as compared to the incommensurate RT monolayer phase. In particular, the Pc ring is more strongly bonded to the surface, which obviously leads to a more planar adsorption of the molecule and, therefore, to higher coherent fractions for N1s and C1s. The smaller distance to the surface is also the reason for the Sn-atoms getting closer to the molecular plane, since they are repulsed by the Ag surface. Therefore, the distance between Sn atom and molecular plane is significantly smaller for a molecule adsorbed in Sn-down position as compared to those in Sn-up position [see Fig. 7(c) and compare Table IV and V]. It can even be speculated, that when the Pc ring comes close to the surface, the space avail-

able for the Sn atom in a Sn-down position is so far reduced that the Sn atoms are forced to evade and occupy the Sn-up position. However, final conclusions can only be drawn when the present results for the commensurate LT structure are compared to the structural properties of the corresponding RT phase, i.e., the disordered submonolayer phase having a coverage equal to the LT phase.

Finally, we want to mention that the LT results obtained from the two crystals are qualitatively equal, but differ quantitatively, which may be due to different coverages (0.87 and 0.78 ML). A coexistence of disordered domains,²⁰ in particular, for the case of the lower coverage (crystal B), cannot be excluded and could lead to (slightly) different average structural parameters.

V. SUMMARY

In summary, we presented precise distances of the C, N, and Sn atoms for two different structures of SnPc on Ag(111), an incommensurate saturated RT monolayer structure with one molecule per unit cell and a commensurate LT submonolayer structure with two molecules per unit cell. In the first case, a general Sn-down configuration of the molecule could be unambiguously concluded from the coherent positions and the high coherent fraction of the Sn absorption profile. A substantial tilt of the molecule could be excluded. We also detected a significant bending of the molecules, indicating that the benzene rings of the molecule also contribute to a chemisorptive bonding. This bonding was found to be even stronger for the second phase, the commensurate LT structure, and might be the reason for the adsorption geometry found for this phase, namely a mixed Sn-up and Sn-down orientation of the molecules. The vertical distances between the atoms in the molecule and the substrate are less different in the commensurate LT structure. We hope that this geometry information of SnPc on Ag(111) improves the understanding of the adsorption and bonding mechanisms of this interesting system and possibly initiates quantum chemical calculations.

ACKNOWLEDGMENTS

The authors acknowledge financial support by the ESRF, Grenoble. We would also like to thank J. Pflaum, University of Stuttgart, Germany, for purifying the SnPc by gradient sublimation. One of us (E.U.) appreciates financial support by the Fonds der Chemischen Industrie.

*Electronic address: stadler@physik.uni-wuerzburg.de

¹S. R. Forrest, Chem. Rev. (Washington, D.C.) **97**, 1793 (1997).

²E. Umbach, M. Sokolowski, and R. Fink, Appl. Phys. A: Mater. Sci. Process. **63**, 565 (1996).

³L. Chkoda, M. Schneider, V. Shklover, L. Kilian, M. Sokolowski, C. Heske, and E. Umbach, Chem. Phys. Lett. **371**, 548 (2003).

⁴F. Schreiber, Phys. Status Solidi A **201**, 1037 (2004).

⁵Y. Hirose, A. Kahn, V. Aristov, P. Soukiassian, V. Bulovic, and S. R. Forrest, Phys. Rev. B **54**, 13748 (1996).

⁶E. V. Tsiper, Z. G. Soos, W. Gao, and A. Kahn, Chem. Phys. Lett. **360**, 47 (2002).

⁷K. Seki, N. Hayashi, H. Oji, E. Ito, Y. Ouchi, and H. Ishii, Thin Solid Films **393**, 298 (2001).

⁸R. Fink, D. Gador, U. Stahl, Y. Zou, and E. Umbach, Phys. Rev. B **60**, 2818 (1999).

⁹U. Baston, M. Jung, and E. Umbach, J. Electron Spectrosc. Relat. Phenom. **77**, 75 (1996).

¹⁰D. Gador, Y. Zou, C. Buchberger, M. Bertram, R. Fink, and E.

- Umbach, J. *Electron Spectrosc. Relat. Phenom.* **103**, 523 (1999).
- ¹¹A. Schöll, Y. Zou, T. Schmidt, R. Fink, and E. Umbach, *J. Phys. Chem. B* **108**, 14741 (2004).
- ¹²Y. Zou, L. Kilian, A. Schöll, T. Schmidt, R. Fink, and E. Umbach, *Surf. Sci.* **600**, 1240 (2006).
- ¹³J. Stanzel, W. Weigand, L. Kilian, H. L. Meyerheim, C. Kumpf, and E. Umbach, *Surf. Sci.* **571**, L311 (2004).
- ¹⁴A. Gerlach, F. Schreiber, S. Sellner, H. Dosch, I. A. Vartanyants, B. C. C. Cowie, T. L. Lee, and J. Zegenhagen, *Phys. Rev. B* **71**, 205425 (2005).
- ¹⁵A. Hauschild, K. Karki, B. C. C. Cowie, M. Rohlfing, F. S. Tautz, and M. Sokolowski, *Phys. Rev. Lett.* **94**, 036106 (2005).
- ¹⁶L. Kilian, W. Weigand, E. Umbach, A. Langner, M. Sokolowski, H. L. Meyerheim, H. Maltor, B. C. C. Cowie, T. Lee, and P. Bäuerle, *Phys. Rev. B* **66**, 075412 (2002).
- ¹⁷F. Allegretti, D. P. Woodruff, V. R. Dhanak, C. Mariani, F. Busolotti, and S. D'Addato, *Surf. Sci.* **598**, 253 (2005).
- ¹⁸J. Zegenhagen, *Surf. Sci. Rep.* **18**, 199 (1993).
- ¹⁹R. G. Jones, A. Chan, M. G. Roper, M. P. Skegg, I. G. Shuttleworth, C. J. Fisher, G. J. Jackson, J. J. Lee, D. P. Woodruff, N. K. Singh, and B. C. C. Cowie, *J. Phys.: Condens. Matter* **14**, 4059 (2002).
- ²⁰S. Hansen, Diploma thesis, Universität Würzburg, 2005.
- ²¹S. Hansen, C. Stadler, C. Kumpf, and E. Umbach (unpublished).
- ²²M. Lackinger and M. Hietschold, *Surf. Sci.* **520**, L619 (2002).
- ²³M. Lackinger, Ph.D. thesis, Technische Universität Chemnitz, 2003.
- ²⁴B. W. Batterman and H. Cole, *Rev. Mod. Phys.* **36**, 681 (1964).
- ²⁵D. P. Woodruff, *Prog. Surf. Sci.* **57**, 1 (1998).
- ²⁶I. A. Vartanyants and J. Zegenhagen, *Phys. Status Solidi B* **215**, 819 (1999).
- ²⁷I. A. Vartanyants and J. Zegenhagen, *Solid State Commun.* **113**, 299 (2000).
- ²⁸J. J. Lee, C. J. Fisher, D. P. Woodruff, M. G. Roper, R. G. Jones, and B. C. C. Cowie, *Surf. Sci.* **494**, 166 (2001).
- ²⁹M. B. Trzhaskovskaya, V. I. Nefedev, and V. G. Yarzhemsky, *Ann. Rheum. Dis.* **77**, 97 (2001).
- ³⁰M. B. Trzhaskovskaya, V. I. Nefedev, and V. G. Yarzhemsky, *Ann. Rheum. Dis.* **82**, 257 (2002).
- ³¹<http://www.ccp3.ac.uk/software.shtml>, program DL_PHASE supplied by the CCP3 secretary A. Wander Daresbury Laboratory, UK as a part of the CCP3 project.
- ³²A. Bechler and R. H. Pratt, *Phys. Rev. A* **39**, 1774 (1989).
- ³³A. Schöll, C. Stadler, C. Kumpf, and E. Umbach (unpublished).